Available online at www.sciencedirect.com

SciVerse ScienceDirect

Ceramics International 39 (2013) 2473–2480

CERAMICS INTERNATIONAL

www.elsevier.com/locate/ceramint

Laser surface modification of plasma sprayed CYSZ thermal barrier coatings

Raheleh Ahmadi-Pidani*, Reza Shoja-Razavi, Reza Mozafarinia, Hossein Jamali*

Department of Materials Engineering, Malek-Ashtar University of Technology, Shahin Shahr, Isfahan, Iran

Received 11 July 2012; received in revised form 1 September 2012; accepted 2 September 2012
Available online 11 September 2012

Abstract

In this study, Inconel 738 LC superalloy coupons were first sprayed with a NiCoCrAlY bond coat and then with a ceria and yttria stabilized zirconia (CYSZ) top coat by air plasma spraying (APS). After that, the plasma sprayed CYSZ thermal barrier coatings (TBCs) were treated using a Nd:YAG pulsed laser. The effect of laser glazing on the microstructure of the coatings was investigated. The microstructures and surface topographies of both as-sprayed and laser glazed samples were investigated using field emission scanning electron microscope (FESEM) and atomic force microscope (AFM). The phases of the coatings were analyzed with X-ray diffractometry (XRD). The microstructural analysis results revealed that laser surface glazing of ceramic top coat reduced the surface roughness considerably, eliminated the surface porosities and produced a network of continuous cracks perpendicular to the surface. XRD patterns also showed that both as-sprayed and laser glazed top coats consisted of nonequibrium tetragonal (T′) phase.

Keywords: Thermal barrier coatings; Laser glazing; CYSZ; Air plasma spraying

1. Introduction

Thermal barrier coatings (TBCs) have been widely used for the protection of gas turbine and diesel engines by reducing heat transfer from combustion gas to the engine components [1,2]. TBCs are powerful tools to enhance engine efficiency and performance [3–5], in terms of higher operating temperatures [6] or lower cooling air flow, as well as lower emissions and lower fuel consumption [4].

A typical TBC system includes MCrAlY (M = Co and/or Ni) metallic bond coat as the oxidation resistant layer and ceramic top coat as the thermal insulation layer [7,8]. The ceramic top coat has a significantly low thermal conductivity, reducing the temperature of the underlying superalloy in relation to the gas path temperature [9,10]. The metallic bond coat is deposited between the metallic substrate and the ceramic top coat to protect the underlying metal from oxidation and high temperature corrosion and enhance the adherence between the dissimilar substrate and the top coat [11–13]. Nowadays, TBCs are usually produced by either air plasma spraying (APS) or electron beam-physical vapor deposition (EB-PVD) [14–16]. However, due to the comparatively cost-effective deposition conditions and high deposition efficiency, plasma spraying technology has found wide acceptance till date [17,18].

The selection of TBC materials is restricted by some basic requirements such as high melting point, no phase transformation between room temperature and operating temperature, low thermal conductivity, chemical inertness, thermal expansion match with metallic substrate, good adherence to metallic substrate and low sintering rate of porous microstructure. Therefore, the number of materials that can be used as TBCs materials is very limited [5]. Yttria stabilized zirconia (YSZ) has been usually chosen for the top coat material because of its high coefficient of thermal expansion (CTE), which closely matches that of the substrate, and low thermal conductivity [19–23]. However, when applied in more demanding environments such as higher temperatures, corrosion and stress were scrutinized

*Corresponding authors. Tel.: +98 31 2522 5041; fax: +98 31 2522 8530.
E-mail addresses: ra-ahmadi@mut-es.ac.ir (R. Ahmadi-Pidani), h.jamali@mut-es.ac.ir (H. Jamali).

0272-8842/$ - see front matter © 2012 Elsevier Ltd and Techna Group S.r.l. All rights reserved.
http://dx.doi.org/10.1016/j.ceramint.2012.09.005

and the ZrO_2-CeO_2-Y_2O_3 (CYSZ) coating appeared to be promising [24,25]. In addition, it has been indicated that the CYSZ coating was superior to the YSZ coating due to its phase stability at high temperature [1,24,25], improved thermal insulation, higher CTE [22,24], good corrosion and thermal shock resistance [24,26].

According to Tsai et al. [27,28], there are two main factors limiting the life of thermal barrier coatings: the oxidation of the bond coat and the thermal mismatch stress. Erosion and corrosion are factors that contribute to the degradation of TBCs and become more important in the presence of high heat flux and a corrosive environment.

Laser treatment is currently recognized as a promising technique for the improvement of plasma sprayed TBCs performance and extension of their lifetime [29–33]. Laser surface modification of YSZ TBCs is associated with reducing surface roughness, sealing open porosity [34,35] and generating a controlled segmented crack network perpendicular to the surface [36,37].

Studies conducted by Tsai and Tsai [38] reported that the use of a pulsed laser prevented defect formation in plasma sprayed ZrO_2–20 wt%Y_2O_3/MCrAlY coatings, which occurred easily with a continuous wave laser. Batista et al. [34] used both Nd:YAG and CO_2 lasers for glazing of 8YSZ coatings. Their results indicated that the crack density was similar in both cases; however, the width of the cracks was substantially smaller in those treated with Nd:YAG laser. Also, voids were found on the surface of the CO_2 laser glazed coatings, while no such case was noticed in those treated with the Nd:YAG laser. Thus, it seems that the pulsed Nd:YAG laser is better for the glazing of zirconia based TBCs than other lasers.

Despite the high potential of laser technology, a few studies have examined the use of laser modification technique in the improvement of plasma sprayed TBCs properties. On the other hand, in this field, up to now, most researches have been conducted on the laser glazing of YSZ coatings. It seems that the evaluation of microstructural changes of CYSZ coatings after laser glazing is a new research area. Therefore, in order to methodically explain the performance of laser glazed CYSZ thermal barrier coatings under various conditions, detailed studies on the microstructure of as-sprayed and laser glazed CYSZ TBCs seem necessary. Hence, this work aims at obtaining the optimum parameters for laser glazing of CYSZ TBCs by using pulsed Nd:YAG laser and characterizing them by comparing them with the as-sprayed ones. This was to acquire a better understanding of the microstructural change produced in CYSZ TBCs by laser surface modification process.

2. Experimental procedures

2.1. Material

Inconel 738 LC superalloy was used as the substrate with the dimension of 16 mm × 16 mm × 10 mm. The ceramic powder of ZrO_2–25 wt%CeO_2–2.5 wt%Y_2O_3 (CYSZ; 205-NS, Sulzer Metco, Westbury, NY, 16–90 μm) as a feedstock for top coat and commercially Ni–23Co–18Cr–6Al-1Y (wt%) metallic powder (22 SN 6883, S.N.M.I.-Avignon, 38–75 μm) as a feedstock for bond coat were air plasma sprayed.

2.2. Air plasma spraying

The thermal barrier coatings, composed of a bond coat (125 ± 25 μm thick) and a top coat (265 ± 25 μm thick), were deposited by air plasma spraying (APS) system. Air plasma spraying was carried out by the Plasma-Technik A3000S system (Sulzer Metco, Wohlen, Switzerland) with a F4-MB plasma gun (Sulzer Metco AG, Winterthur, Switzerland). The substrates were grit blasted, degreased and cleaned with acetone and preheated with plasma gun prior to spraying. The measured surface roughness (R_a) of substrates was 9.20 μm. During the spraying process, a cooling system (air blowing) was applied to reduce the coatings temperature. In the authors' previous study [39], desirable CYSZ TBCs were obtained and appropriate spraying parameters were suggested.

2.3. Laser treatment

The coated samples surfaces were laser treated by a Nd:YAG pulsed laser, model IQL-10 with mean power of 400 W and standard square shaped pulses. After determining optimum parameters, the final samples were placed on the x–y table and the laser beam was scanned over the specimen surfaces, generating multiple parallel tracks of controlled overlapping to treat the whole surface area of the coatings.

Since the microstructure and quality of the glazed layer play an important role in the performance of TBCs, it is very important to select suitable laser parameters. In order

Table 1
Laser glazing parameters.

Parameter	Series 1	Series 2	Series 3	Series 4	Series 5
Average power (W)	200	160	120	120	80
Pulse frequency (Hz)	40	40	30	30	20
Scanning speed (mm/s)	6.67	10	20	20	20
Argon flow rate (SLPM*)	10	10	10	10	10

*Standard Liter Per Minute.

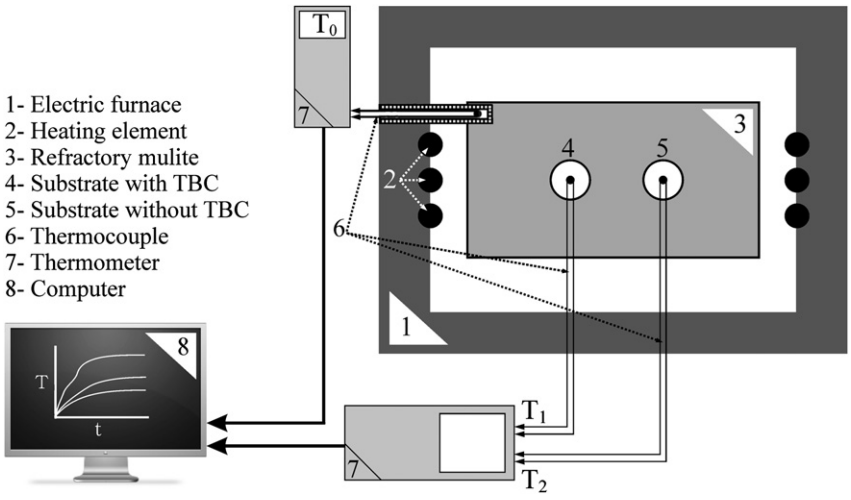

Fig. 1. Schematic illustration of thermal insulation capability test.

to determine optimum parameters, several series of parameters were used. These parameters are summarized in Table 1. Optimum parameters were selected based on melted depth and surface quality of the glazed layer.

2.4. Thermal insulation capability test

To evaluate thermal insulation value of TBCs, the thermal insulation capability test was designed and administered. The schematic illustration of thermal insulation capability test is shown in Fig. 1. To implement the test, electric furnace door with a refractory mulite was replaced. The substrate was coated with TBC so that coated surface inside furnace and substrate backsides in air, embedded within the refractory mulite. In order to eliminate the effects of temperature drop by substrate, cooling the substrate backside by the air and instrumental errors, a similar substrate without TBC was used as voucher sample. Open spaces between the refractory/furnace and refractory/sample were closed using high temperature sealant. Three thermocouples were used as sensors, one was located in the furnace to measure the furnace temperatures (T_0) and others were sealed on both sample backsides to monitor the backside temperatures of the coated sample (T_1) and voucher sample (T_2). The thermocouples were linked to thermometer and then computer to record the heating temperature curves (T_0, T_1 and T_2). After installation, the electric furnace was heated to 1000 °C with the average rate of 15 °C/min. To stabilize temperature conditions, the samples were kept at 1000 °C for 40 min. T_0, T_1 and T_2 record from the beginning of the test in one minute time intervals and t–T curves were plotted. Finally, the thermal insulation capability by the temperature drop across TBC ($\Delta T = T_2 - T_1$) for twenty-end data was calculated. A test similar to this test has also been performed by Gong et al. [22].

2.5. Characterization

The microstructural characteristics of as-sprayed and laser glazed coatings were investigated by a field emission scanning electron microscope (FESEM; S-4160, Hitachi Ltd., Japan). Surface topography of as-sprayed and laser glazed coatings was evaluated by atomic force spectroscope (AFM; DME Dualscope DS-95-200-E, Denmark; 0.12 nN, 30 μm/s). Phase analysis has been carried out with the use of X-ray diffractometry (XRD; Bruker-D8 ADVANCE, Germany; 40 kV, 40 mA, Cu-Kα radiation). The surface roughness (R_a) of as-sprayed and laser glazed coatings was measured by a roughness tester (Mitutoyo SJ-201P, Japan). The roughness reported was the average of five values scanned from different areas on coating surface.

3. Results and discussion

3.1. Microstructure of as-sprayed coating

Fig. 2 shows the FESEM micrograph of top surface of as-sprayed CYSZ coating. It can be seen that top surface of coating is very rough because it includes splats (molten particles deformed on impact into a pancake shape) that are deposited on surface with different felattening parameters. Enclosing transverse microcracks are also visible. Fig. 3 shows the fractured cross section of plasma sprayed CYSZ coating. The coating exhibited a layered structure including splats that are placed on each other. As can be seen, in this figure, the structure within each splat is crystalline with well-defined columnar grains. Also, the presence of inter-splat cracks and porosities is evident. The formation of these defects is attributed to random deposition, residual stresses during the deposition process, the lack of complete overlap of adjacent splats and gas entrapment during the deposition process [40]. This is a common feature of plasma sprayed ceramic coatings, reducing thermal conductivity and also affecting mechanical properties of the coatings. However, these pores and microcracks inevitably provide infiltration paths for molten salts to attack the coating [41].

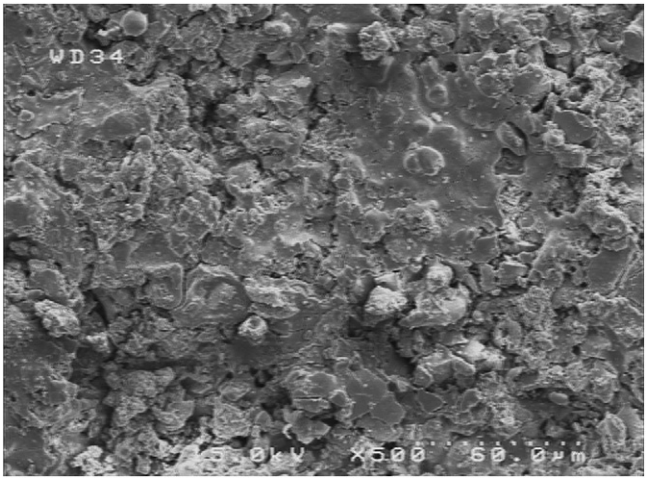

Fig. 2. FESEM micrograph of top surface of as-sprayed CYSZ coating.

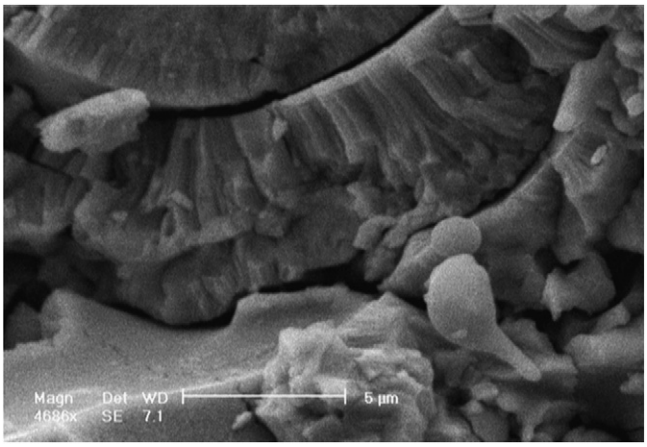

Fig. 3. SEM micrograph of fractured cross section of plasma sprayed ceramic top coat.

3.2. Determination of optimum laser treatment parameters

Optimum parameters of laser surface modification were determined based on thickness and surface quality of the glazed layer. Therefore, the average thickness of treated layer should be as low as possible so that the minimum microstructural changes occur and only a thin dense layer is formed on the surface of top coat. Moreover, the crack network produced by laser processing must be regular. This is expected to be beneficial for accommodating the oxidation stress and mismatch stress.

Fig. 4(a) shows the FESEM micrograph of the cross section of first sample laser treated by first series of parameters. As shown, the average thickness of molten layer is 750 μm at top coat, while the bond coat and a part of substrate were melted. Moreover, the surface of glazed layer was rough, containing an irregular network of cracks. Therefore, for melt depth reduction, scan speed and nozzle distance from the surface were increased and laser power was decreased as compared to first series of parameters. According to Fig. 4(b), the average thickness of molten layer was obtained which was around 165 μm by second series of parameters. As can be seen, a large part of top coat was melted and the crack network produced on the surface was very irregular. Therefore, these parameters were not suitable and then the treatment was performed by third series of parameters. Accordingly, laser power and pulse frequency were decreased and scan speed and nozzle distance from the surface were increased more than second series of parameters. However, the average thickness of the molten layer was also high and a large part of top coat was melted. In addition, surface cracks were partly irregular. This is shown in Fig. 4(c). In the fourth step, only nozzle distance from the surface was increased more than the previous parameters. As shown in Fig. 4(d), the average thickness of molten layer was obtained which was around 58 μm. As can be seen, the crack network produced on the surface was more regular than the previous steps, but melting depth was higher than the desirable value. Thus, in order to obtain the suitable molten depth, laser power and pulse frequency were still less. According to Fig. 4(e), by using fifth series of parameters, the average thickness of molten layer was obtained which was around 30 μm and the crack network was very regular. In addition, there was no defect on the surface of the sample. Therefore, fifth series of parameters with 20% overlap were selected as the operating parameters for laser surface modification of plasma sprayed CYSZ thermal barrier coatings. The melting depth for various parameter series is graphically presented in Fig. 5.

3.3. Microstructure of laser glazed coating

Laser glazing effects on the microstructure of as-sprayed coatings are described below.

3.3.1. Surface roughness reduction

Fig. 6 shows the top surface of laser glazed coating. It can be seen that rough and irregular surface of as-sprayed coating (Fig. 2) was changed to smooth and flat surface after laser glazing process. Fig. 7 shows the AFM micrographs of as-sprayed and laser glazed coating surfaces. It confirms considerable reduction of the surface roughness after laser glazing process. In laser surface modification process, laser beam was radiated on the surface, remelting it by high heat creation. When the laser beam passed through the molten area, this zone was solidified rapidly. These remelting and resolidification phenomena resulted in the reduction of surface roughness of plasma sprayed coating. The measured surface roughness (R_a) of laser glazed coating (2.20 μm) and as-sprayed coating (7.58 μm) also confirms this reduction. According to the previous studies [35,36], considerable reduction in the surface roughness leads to the improvement of the erosion. Also, due to the reduction of specific surface area of the glazed

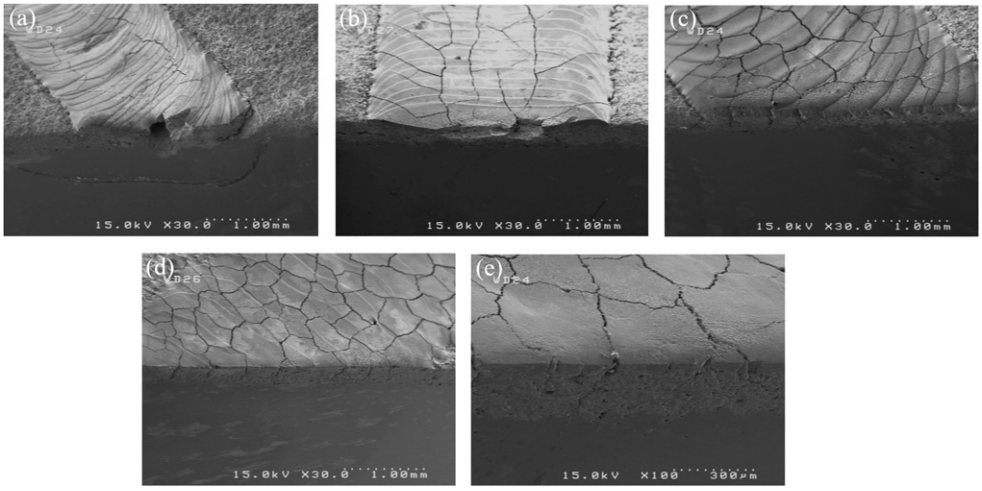

Fig. 4. Cross section FESEM micrographs of laser treated sample by (a) first, (b) second, (c) third, (d) fourth and (e) fifth series of parameters.

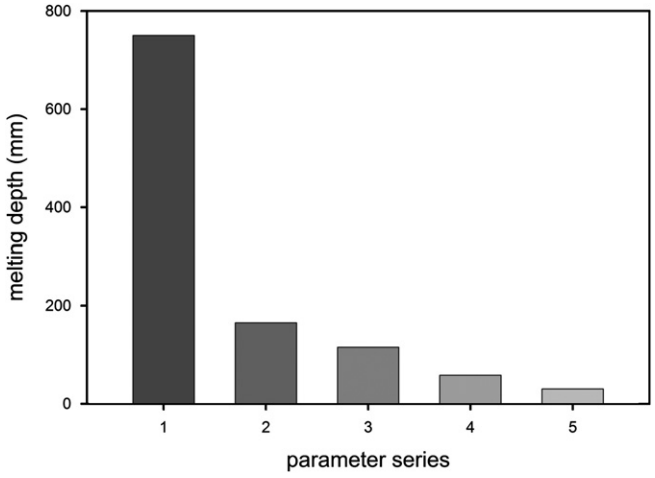

Fig. 5. Melting depth for various parameter series.

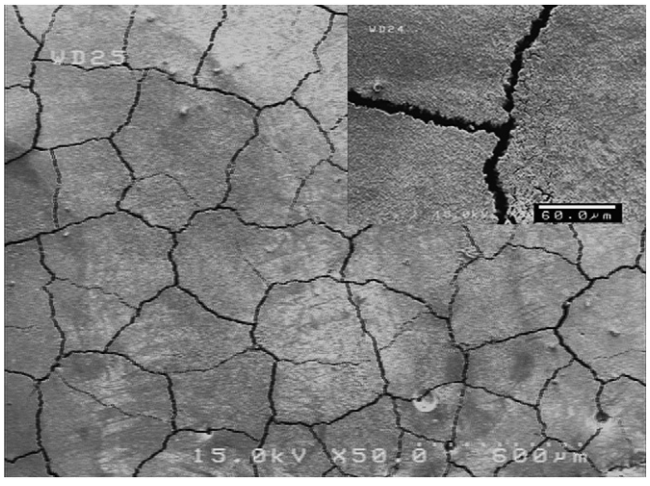

Fig. 6. FESEM micrographs of top surface of laser glazed coating.

layer, the corrosion reaction of the molten salts with the top coat will be reduced as compared with the coatings in the as-sprayed condition [34].

3.3.2. Segmented cracks generation

Based on Fig. 6, a continuous network of segmented cracks is visible on the surface. Fig. 8 shows the FESEM micrograph of fractured cross section of laser glazed coating. As shown, the glazed layer had segmented cracks perpendicular to the surface. Accordingly, the thickness of the glazed layer was 25–30 μm and the segmented cracks would extend throughout the remelted layer thickness. The formation of segmented cracks is attributed to shrinkage and relaxation of residual stresses during the rapid and nonuniform cooling of molten zirconia [36,37] and probably to the large and localized temperature gradient which generates residual stresses after the laser has passed [36]. The segment cracks are expected to be beneficial for accommodating the oxidation stress, mismatch stress, and the increased thermal shock resistance of TBCs [24,34].

3.3.3. Sealing open porosity

High magnification micrograph of the glazed layer is shown in Fig. 9. As can be seen, the laser glazed layer had a dense microstructure and the as-sprayed structure porosities were eliminated due to remelting and resolidification. Sealing open porosities and creating dense microstructure result in the improvement of the hot corrosion resistance of zirconia based TBCs by preventing molten salt penetration into the coating. This is in accordance with the results obtained in the previous works [27,28,34]. In addition, the microholes formed due to the gasification and the bubbles formed during the melting are not evident in the melt region (Fig. 9). This is mainly because of the low scanning speed of the laser beam; consequently, bubbles formed during the laser melting coalesce and escape during melting and voids formed by the bubbles are filled with liquid due to the surface tension force [33].

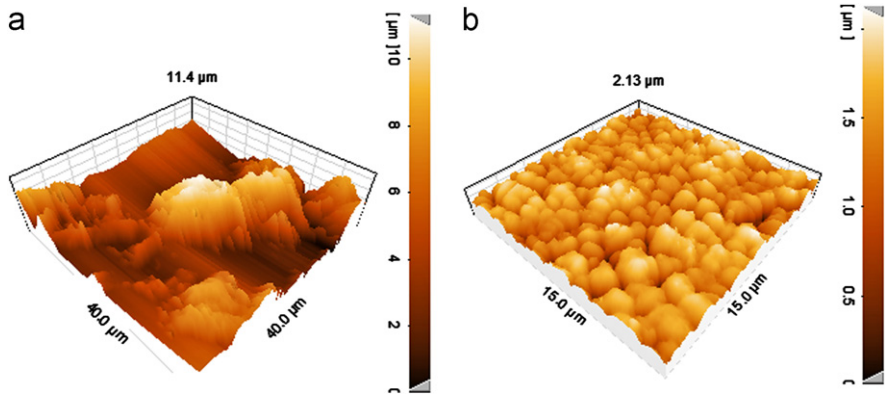

Fig. 7. AFM images of as-sprayed (a) and laser glazed (b) coatings surfaces.

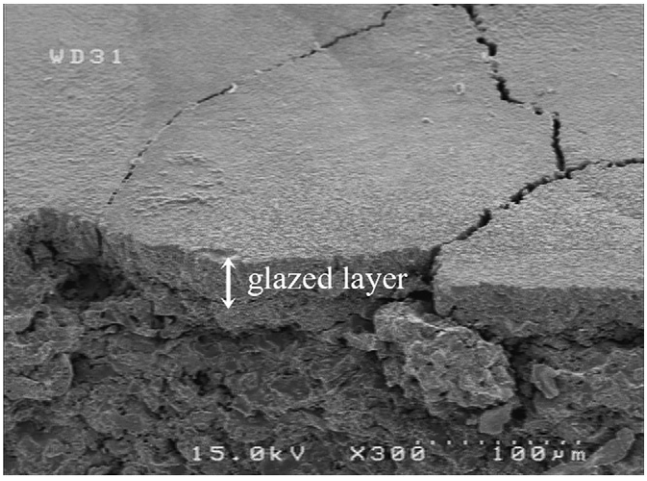

Fig. 8. FESEM micrograph of fractured cross section of laser glazed coating.

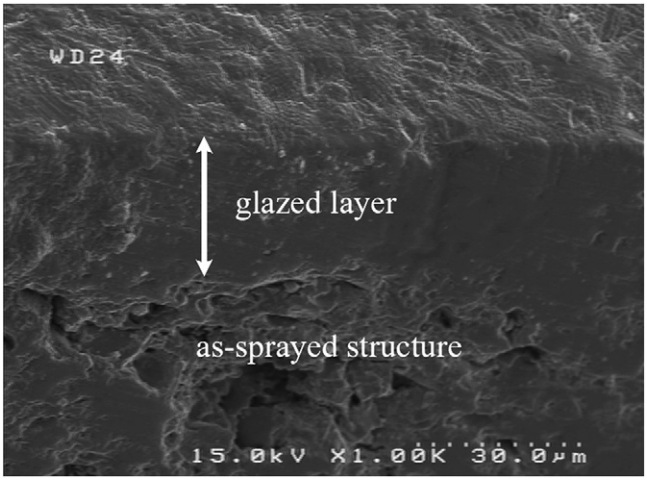

Fig. 9. High magnification FESEM micrograph of laser glazed layer.

3.4. Phase analysis of coatings

The XRD patterns of as-sprayed and laser glazed coatings are shown in Fig. 10. As can be seen, both coatings

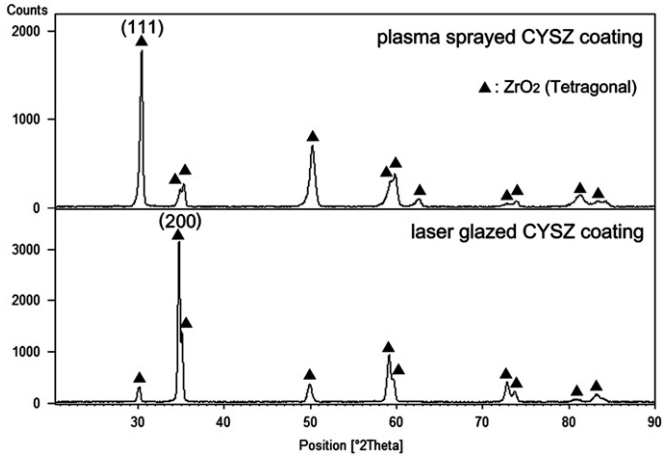

Fig. 10. XRD patterns of as-sprayed and laser glazed CYSZ coatings.

consisted of tetragonal (T′) phase. T′ phase is a kind of non-equilibrium phase formed due to the rapid cooling at room temperature [42,43]. The cooling rate of the splats during the plasma spraying process was estimated to be higher than 10^7 °C s^{-1} and the estimated cooling rate of the glazed layer is about 10^3-10^4 °C s^{-1} [24]. Therefore, the presence of zirconia in the T′ phase after plasma spraying and laser glazing is a common subject approved by other researches too [22,41]. The relative peak intensity of as-sprayed coating is similar to data from JCPDS-00-017-0923 card whereas the laser glazed coating revealed the highest (200) peak intensity. This implied that the laser glazed coating exhibited a preferred orientation of [100] direction. More discussion on this subject needs further investigations and is not within the scope of this paper.

3.5. Thermal insulation capability

The main task of the TBCs is to reduce the transfer of thermal energy to the hot section of metal components. Therefore, the thermal insulation capability is considered as one of the most significant factors for evaluating the performance of TBCs. In this study, the thermal insulation capability of TBCs was evaluated by the temperature drop

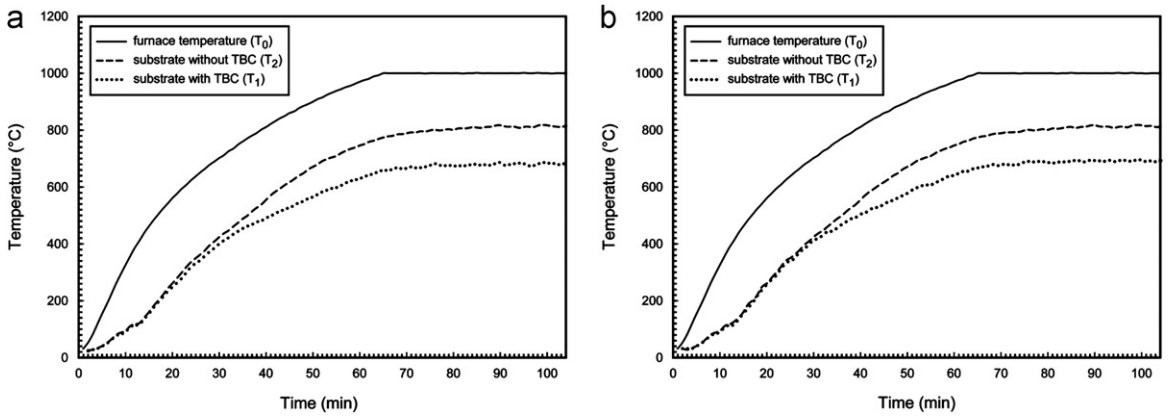

Fig. 11. Heating temperature curves of furnace and samples: as-sprayed TBC (a) and laser glazed TBC (b).

across TBCs. Based on the results (Fig. 11), thermal insulation capability for as-sprayed and laser glazed CYSZ TBCs was found to be 132 °C and 121 °C, respectively. This demonstrates that the thermal insulation capability of the laser glazed TBC, as compared to the as-sprayed TBC, was around 8% lower.

The ability of thermal insulation of plasma sprayed CYSZ coatings is attributed to the characteristics of crystal structure and microstructure, which result from the spraying process. Generally, in the ceramic materials, the lattice vibration controls thermal conductivity by scattering of phonons and thereby hindering the transportation of phonons. Adding stabilizers to the crystal structure of zirconia led to the creation of O^{2-} vacancies and local strain fields in the lattice structure. These vacancies and strain fields directly increase phonon scattering in the lattice [40]. On the other hand, the microstructure of plasma sprayed TBCs contains a network of microcracks and porosities, providing low thermal conductivity through thickness [42,44].

In laser glazed TBCs, a little part of layered structure of top coat, including microcracks and porosities, was alternated with the dense structure. Therefore, little reduction in thermal insulation capability can be attributed to this microstructural change, which is the most effective reason for improvement of erosion, corrosion and thermal shock resistance of TBCs.

4. Conclusion

The CYSZ thermal barrier coatings were produced by air plasma spraying. Optimum parameters for laser surface modification of plasma sprayed CYSZ thermal barrier coatings by pulsed Nd:YAG laser were obtained. The microscopic observation showed that laser glazing process reduced the surface roughness considerably, eliminated the surface porosity and produced a network of continuous cracks perpendicular to the surface. Both as-sprayed and laser glazed coatings consisted of tetragonal (T′) phase. The thermal insulation capability of the laser glazed TBC, as compared to the as-sprayed TBC, was slightly lower due to microstructural change in the thin layer of top coat. However, it is expected that the microstructural changes resulting from laser surface modification lead to the improvement of the resistance to erosion, corrosion and thermal shock of plasma sprayed CYSZ TBCs.

Acknowledgment

The authors wish to acknowledge Malek-Ashtar University of Technology for support of this study. The authors would also like to thank Hossein Zamani and Zia Valefi for their cooperation.

References

[1] G.D. Girolamo, C. Blasi, M. Schioppa, L. Tapfer, Structure and thermal properties of heat treated plasma sprayed ceria–yttria co-stabilized zirconia coatings, Ceramics International 36 (2010) 961–968.
[2] S. Das, S. Datta, D. Basu, G.C. Das, Thermal cyclic behavior of glass-ceramic bonded thermal barrier coating on nimonic alloy substrate, Ceramics International 35 (2009) 2123–2129.
[3] N. Wang, C. Zhou, S. Gong, H. Xu, Heat treatment of nanostructured thermal barrier coating, Ceramics International 33 (2007) 1075–1081.
[4] G.D. Girolamo, C. Blasi, L. Pagnotta, M. Schioppa, Phase evolution and thermophysical properties of plasma sprayed thick zirconia coatings after annealing, Ceramics International 36 (2010) 2273–2280.
[5] C.S. Ramachandran, V. Balasubramanian, P.V. Ananthapadmanabhan, V. Viswabaskaran, Influence of the intermixed interfacial layers on the thermal cycling behaviour of atmospheric plasma sprayed lanthanum zirconate based coatings, Ceramics International 38 (5) (2012) 4081–4096.
[6] C.K. Roy, M. Noor-A-Alam, A.R. Choudhuri, C.V. Raman, Synthesis and microstructure of Gd_2O_3-doped HfO_2 ceramics, Ceramics International 38 (2012) 1801–1806.
[7] L. Wang, Y. Wang, X.G. Sun, J.Q. He, Z.Y. Pan, C.H. Wang, Thermal shock behavior of 8YSZ and double-ceramic-layer La2Zr_2O_7/8YSZ thermal barrier coatings fabricated by atmospheric plasma spraying, Ceramics International 38 (5) (2012) 3595–3606.
[8] Q. Yu, A. Rauf, Na Wang, C. Zhou, Thermal properties of plasma-sprayed thermal barrier coating, with bimodal structure, Ceramics International 37 (2011) 1093–1099.

[9] Y. Li, Y. Xie, L. Huang, X. Liu, X. Zheng, Effect of physical vapor deposited Al_2O_3 film on TGO growth in YSZ/CoNiCrAlY coatings, Ceramics International 38 (6) (2012) 5113–5121.
[10] Y. Wang, G. Sayre, Commercial thermal barrier coatings with a double-layer bond coat on turbine vanes and the process repeatability, Surface and Coatings Technology 203 (2009) 2186–2192.
[11] M. Alfano, G.D. Girolamo, L. Pagnotta, D. Sun, Processing, microstructure and mechanical properties of air plasma-sprayed ceria–yttria co-stabilized zirconia coatings, Strain 46 (2010) 409–418.
[12] S. Das, S. Datta, D. Basu, G.C. Das, Glass-ceramics as oxidation resistant bond coat in thermal barrier coating system, Ceramics International 35 (2009) 1403–1406.
[13] R. Vaßen, M.O. Jarligo, T. Steinke, D.E. Mack, D. Stöver, Overview on advanced thermal barrier coatings, Surface and Coatings Technology 205 (2010) 938–942.
[14] J. Fenech, C. Viazzi, J. Bonino, F. Ansart, A. Barnabe, Morphology and structure of YSZ powders: comparison between xerogel and aerogel, Ceramics International 35 (2009) 3427–3433.
[15] S. Guo, Y. Kagawa, Effect of thermal exposure on hardness and Young's modulus of EB-PVD yttria-partially-stabilized zirconia thermal barrier coatings, Ceramics International 32 (2006) 263–270.
[16] R.W. Steinbrech, V. Postolenko, J. Monch, J. Malzbender, L. Singheiser, Testing method to assess lifetime of EB-PVD thermal barrier coatings on tubular specimens in static and cyclic oxidation tests, Ceramics International 37 (2011) 363–368.
[17] X. Chen, Y. Zhao, X. Fan, Y. Liu, B. Zou, Y. Wang, H. Ma, X. Cao, Thermal cycling failure of new $LaMgAl_{11}O_{19}$/YSZ double ceramic top coat thermal barrier coating systems, Surface and Coatings Technology 205 (2011) 3293–3300.
[18] Y. Bai, Z.H. Han, H.Q. Li, C. Xu, Y.L. Xu, Z. Wang, C.H. Ding, J.F. Yang, High performance nanostructured ZrO_2 based thermal barrier coatings deposited by high efficiency supersonic plasma spraying, Applied Surface Science 257 (2011) 7210–7216.
[19] H. Jamali, R. Mozafarinia, R. Shoja-Razavi, R. Ahmadi-Pidani, Comparison of thermal shock resistances of plasma-sprayed nanostructured and conventional yttria stabilized zirconia thermal barrier coatings, Ceramics International 38 (2012) 6705–6712.
[20] H. Jamali, R. Mozafarinia, R. Shoja-Razavi, R. Ahmadi-Pidani, Investigation of thermal shock behavior of plasma-sprayed NiCoCrAlY/YSZ thermal barrier coatings, Advanced Materials Research 472–475 (2012) 246–250.
[21] M. Saremi, A. Afrasiabi, Akira Kobayashi, Microstructural analysis of YSZ and YSZ/Al_2O_3 plasma sprayed thermal barrier coatings after high temperature oxidation, Surface and Coatings Technology 202 (2008) 3233–3238.
[22] W.B. Gong, C.K. Sha, D.Q. Sun, W.Q. Wang, Microstructures and thermal insulation capability of plasma-sprayed nanostructured ceria stabilized zirconia coatings, Surface and Coatings Technology 201 (2006) 3109–3115.
[23] H. Jamali, R. Ahmadi-Pidani, R. Mozafarinia, R. Shoja-Razavi, H. Zamani, Proceedings of the 12th National Conference on Surface Engineering, Malek-Ashtar University of Technology, Shahinshahr, Iran, 10–12 May 2011, pp. 172–181.
[24] J.H. Lee, P.C. Tsai, C.L. Chang, Microstructure and thermal cyclic performance of laser-glazed plasma-sprayed ceria–yttria-stabilized zirconia thermal barrier coatings, Surface and Coatings Technology 202 (2008) 5607–5612.
[25] R. Ahmadi-Pidani, R. Shoja-Razavi, R. Mozafarinia, H. Jamali, Comparison of hot corrosion resistance of YSZ and CYSZ thermal barrier coatings in presence of sulfate–vanadate molten salts, Advanced Materials Research 472–475 (2012) 141–144.
[26] R. Ahmadi-Pidani, H. Jamali, R. Shoja-Razavi, R. Mozafarinia, H. Zamani, Proceedings of the 12th National Conference on Surface Engineering, Malek-Ashtar University of Technology, Shahinshahr, Iran, 10–12 May 2011, pp. 658–667.
[27] P.C. Tsai, C.S. Hsu, High temperature corrosion resistance and microstructural evaluation of laser-glazed plasma-sprayed zirconia/MCrAlY thermal barrier coatings, Surface and Coatings Technology 183 (2004) 29–34.
[28] P.C. Tsai, J.H. Lee, C.S. Hsu, Hot corrosion behavior of laser-glazed plasma-sprayed yttria-stabilized zirconia thermal barrier coatings in the presence of V_2O_5, Surface and Coatings Technology 201 (2007) 5143–5147.
[29] P.C. Tsai, J.H. Lee, C.L. Chang, Improving the erosion resistance of plasma-sprayed zirconia thermal barrier coatings by laser glazing, Surface and Coatings Technology 202 (2007) 719–724.
[30] X. Wang, P. Xiao, M. Schmidt, L. Li, Laser processing of yttria stabilised zirconia/alumina coatings on Fecralloy substrates, Surface and Coatings Technology 187 (2004) 370–376.
[31] H. Chen, Y. Hao, H. Wang, W. Tang, Analysis of the microstructure and thermal shock resistance of laser glazed nanostructured zirconia TBCs, Journal of Thermal Spray Technology 19 (3) (2010) 558–565.
[32] M.F. Morks, C.C. Berndt, Y. Durandet, M. Brandt, J. Wang, Microscopic observation of laser glazed yttria-stabilized zirconia coatings, Applied Surface Science 256 (2010) 6213–6218.
[33] R. Ahmadi-Pidani, R. Shoja-Razavi, R. Mozafarinia, H. Jamali, Improving the thermal shock resistance of plasma sprayed CYSZ thermal barrier coatings by laser surface modification, Optics and Lasers in Engineering 50 (2012) 780–786.
[34] C. Batista, A. Portinha, R.M. Ribeiro, V. Teixeira, C.R. Oliveira, Evaluation of laser-glazed plasma-sprayed thermal barrier coatings under high temperature exposure to molten salts, Surface and Coatings Technology 200 (2006) 6783–6791.
[35] C. Batista, A. Portinha, R.M. Ribeiro, V. Teixeira, M.F. Costa, C.R. Oliveira, Morphological and microstructural characterization of laser-glazed plasma-sprayed thermal barrier coatings, Surface and Coatings Technology 200 (2006) 2929–2937.
[36] C. Batista, A. Portinha, R.M. Ribeiro, V. Teixeira, M.F. Costa, C.R. Oliveira, Surface laser-glazing of plasma-sprayed thermal barrier coatings, Applied Surface Science 247 (2005) 313–319.
[37] G. Zhang, Y. Liang, Y. Wu, Z. Feng, B. Zhang, F. Liu, Laser remelting of plasma sprayed thermal barrier coatings, Journal of Materials Science and Technology 17 (2001) 105–110.
[38] H.L. Tsai, P.C. Tsai, Laser glazing of plasma-sprayed zirconia coatings, Journal of Materials Engineering and Performance 7 (2) (1998) 258–264.
[39] R. Ahmadi-Pidani, R. Shoja-Razavi, H. Jamali, R. Mozafarinia, Evaluation of hot corrosion behavior of plasma sprayed ceria and yttria stabilized zirconia thermal barrier coatings in the presence of $Na_2SO_4+V_2O_5$ molten salt, Ceramics International 38 (2012) 6613–6620.
[40] H. Jamali, R. Mozafarinia, R. Shoja Razavi, R. Ahmadi-Pidani, M.R. Loghman-Estarki, Fabrication and evaluation of plasma-sprayed nanostructured and conventional YSZ thermal barrier coatings, Current Nanoscience 8 (3) (2012) 402–409.
[41] X.H. Zhong, Y.M. Wang, Z.H. Xu, Y.F. Zhang, J.F. Zhang, X.Q. Cao, Hot-corrosion behaviors of overlay-clad yttria-stabilized zirconia coatings in contact with vanadate–sulfate salts, Journal of the European Ceramic Society 30 (2010) 1401–1408.
[42] S. Bose, High Temperature Coatings, first ed., Elsevier Science & Technology Books, USA, 2007.
[43] R.S. Lima, A. Kucuk, C.C. Berndt, Integrity of nanostructured partially stabilized zirconia after plasma spray processing, Materials Science and Engineering A 313 (2001) 75–82.
[44] I.O. Golosnoy, A. Cipitria, T.W. Clyne, Heat transfer through plasma-sprayed thermal barrier coatings in gas turbines: a review of recent work, Journal of Thermal Spray Technology 18 (5–6) (2009) 809–821.